



# MSCs seeded on bioengineered scaffolds improve skin wound healing in rats

Lucia Formigli, BSc\*<sup>1</sup>; Ferdinando Paternostro, MD<sup>1</sup>; Alessia Tani, BSc<sup>1</sup>; Carlo Mirabella, MD<sup>3</sup>; Alessandro Quattrini Li, MD<sup>2</sup>; Daniele Nosi, BSc<sup>1</sup>; Federica D'Asta, MD<sup>5</sup>; Riccardo Saccardi, MD<sup>4</sup>; Benedetta Mazzanti, BSc<sup>4</sup>; Giulia Lo Russo, MD<sup>2</sup>; Sandra Zecchi-Orlandini, BSc<sup>1</sup>

1. Department of Experimental and Clinical Medicine, Section of Anatomy and Histology,
2. Department of Surgery and Translational Medicine, University of Florence,
3. Immunohaematology and Transfusion Medicine,
4. Department of Haematology, Cord Blood Bank, University Hospital of Careggi, Florence, Italy
5. Burn Centre, Birmingham Children Hospital, Birmingham, United Kingdom

## Reprint requests:

Prof. Sandra Zecchi-Orlandini, Department of Experimental and Clinical Medicine, Section of Anatomy and Histology, University of Florence, L.go Brambilla 3, Florence 50134, Italy.  
Tel: +39 0552758070;  
Fax: +39 0554379500;  
Email: zecchi@unifi.it

\*This paper is dedicated to the dear memory of Lucia Formigli who passed away on March 18, 2014.

Manuscript received: February 11, 2014  
Accepted in final form: December 12, 2014

DOI:10.1111/wrr.12251

## ABSTRACT

Growing evidence has shown the promise of mesenchymal stromal cells (MSCs) for the treatment of cutaneous wound healing. We have previously demonstrated that MSCs seeded on an artificial dermal matrix, Integra (Integra Lifesciences Corp., Plainsboro, NJ) enriched with platelet-rich plasma (Ematrix) have enhanced proliferative potential in vitro as compared with those cultured on the scaffold alone. In this study, we extended the experimentation by evaluating the efficacy of the MSCs seeded scaffolds in the healing of skin wounds in an animal model in vivo. It was found that the presence of MSCs within the scaffolds greatly ameliorated the quality of regenerated skin, reduced collagen deposition, enhanced reepithelization, increased neo-angiogenesis, and promoted a greater return of hair follicles and sebaceous glands. The mechanisms involved in these beneficial effects were likely related to the ability of MSCs to release paracrine factors modulating the wound healing response. MSC-seeded scaffolds, in fact, up-regulated matrix metalloproteinase 9 expression in the extracellular matrix and enhanced the recruitment of endogenous progenitors during tissue repair. In conclusion, the results of this study provide evidence that the treatment with MSC-seeded scaffolds of cutaneous wounds contributes to the recreation of a suitable microenvironment for promoting tissue repair/regeneration at the implantation sites.

Bone marrow-derived mesenchymal stromal cells (MSCs) generate great expectation in the field of regenerative medicine due to the easy isolation and expansion, unique anti-inflammatory and immune-modulatory properties, and their potential multipotency.<sup>1-4</sup> These cells have been successfully used in cell-based therapies for cutaneous regeneration experiments and, recently, clinically explored for improving burn healing and reepithelialization of chronic ulcerated skin.<sup>5,6</sup> However, the detailed mechanisms of the beneficial effects of these cells are far from being clarified and must be elucidated before MSCs could be widely transferred from the bench to the bedside. Several recent reports suggest that differentiation or transdifferentiation of MSCs is involved in wound healing of skin and appendages;<sup>7-9</sup> their differentiation into multiple skin cell types has been confirmed by the expression of specific epidermal markers, including cytokeratin and filaggrin.<sup>10,11</sup> Other researchers have, instead, distinct opinion, suggesting that MSCs participate in skin repair/regeneration in the absence of a significant long-term engraftment through the secretion of paracrine factors that stimulate survival, proliferation, migration, and differentiation of the resident cells.<sup>12-16</sup> In particular, enzyme-linked immunosorbent assay has shown that conditioned medium from MSCs contains a wide variety of growth factors and

cytokines, such as epidermal growth factor, fibroblast growth factor (FGF), vascular endothelial growth factor (VEGF), IL-6, IL-8, plus fibrinolytic enzymes and matrix metalloproteinases (MMPs), which may influence cellular activities in the wound microenvironment and consequently regulate the reparative quality outcome.<sup>17-21</sup> Indeed, VEGF and FGF have been reported to prime neo-angiogenesis by stimulating endothelial precursors to migrate and aggregate into primary capillary plexus,<sup>22</sup> and the up-regulated expression of MMPs, a family of enzymes that selectively digests individual components of ECM, exerts an antifibrotic effect through the inhibition of excessive collagen deposition at wound sites.<sup>23,24</sup> This latter effect, in turn, may permit cell migration and the restoration of tissue continuity. On the other hand, fibrosis of the skin represents a major symptomatic

FGF	Fibroblast growth factor
GFP	Green fluorescent protein
MMP9	Matrix metalloproteinase 9
MSCs	Mesenchymal stromal cells
PRP	Platelet-rich plasma
VEGF	Vascular endothelial growth factor

clinical issue because it can lead to the formation of abnormal scar (such as hypertrophic scarring and keloids), which causes significant problems in tissue growth, function, and aesthetics.<sup>25–27</sup>

On these bases, most of the current research is now directed to the identification of appropriate scaffolds with suitable biomechanical properties to support MSCs' viability and growth in the hostile wound microenvironment and retain them at the desired location, thus enhancing their trophic activity on the host tissue.<sup>28,29</sup> In this line, we have previously demonstrated the good potential for using MSCs via tissue-engineered constructs by showing that the combination of an artificial dermal matrix, Integra (Integra Lifesciences Corp., Plainsboro, NJ), with platelet-rich plasma (PRP) (Ematrix) may represent a promising approach to optimize MSC engraftment in cutaneous wounds.<sup>30</sup> In the present study, we wanted to test the therapeutic efficacy *in vivo* of this peculiar substrate for skin regeneration. To this purpose, MSCs isolated from green fluorescent protein (GFP) transgenic rats were seeded on Integra matrix adsorbed or not with PRP and then implanted into prepared wounds on the dorsum of rats. The scaffolds without cells were implanted on the other side of the dorsum. The results of our study contribute to clarify the mechanisms underlying the therapeutic benefits of MSCs for skin repair/regeneration, suggesting that these cells, when seeded into the bioengineered scaffold Integra + PRP (Ematrix), are able to ameliorate the quality of tissue repair and contribute to skin regeneration through paracrine mechanisms.

## MATERIALS AND METHODS

### Ethics statement

All animal manipulations were carried out according to the European Community guidelines for animal care (DL 116/92, application of the European Communities Council Directive of 24 November 1986; 86/609/EEC) and approved by the Committee for Animal Care and Experimental Use of the University of Florence. The experimental procedures were authorized by Italian Ministry of Health (215/2012—B) according to the Italian law (Art.7/D.lgs 116/92). The animals were housed with free access to food and water and maintained on a 12-hour light/dark cycle at 22 °C room temperature (RT). All efforts were made to minimize the animal suffering and the number of animals sacrificed.

### Experimental animals

Eighteen male Lewis rats (8-week old) (Harlan Laboratories, Correzzana-Monza, Italy), weighing  $250 \pm 20$  g, were anesthetized with 4% chloral hydrate (40 mg/Kg) via intraperitoneal injection. After having shaved and cleaned with chlorhexidine 2%, two rectangles (one for each side,  $2 \times 4$  cm) were outlined with a permanent marker on the dorsum of the rats. The incisions were made along the marked edges reaching the subcutaneous layer, and the overlying skin was excised. The animals were randomly divided into three groups of six animals each:

- Control animals, undergoing surgery and left to heal spontaneously;
- Animals treated with Integra matrix ( $2 \times 4$  cm) on the left side and Integra matrix ( $2 \times 4$  cm) seeded with rat

- GFP-labeled MSCs ( $1 \times 10^6$  cells) on the right side; and
- Animals treated with Ematrix ( $2 \times 4$  cm adsorbed with 1.2 mL of PRP) on the left side and Ematrix seeded with rat GFP-labeled MSC ( $2 \times 4$  cm adsorbed with 1.2 mL of PRP +  $1 \times 10^6$  cells) on the right side.

Integra matrix and Ematrix were fixed to the skin using 5-0 Monocryl surgical suture (Ethicon Inc., Somerville, NJ). The wounds were then covered with a gauze containing silver salts (Acticoat, Smith & Nephew, Hull, United Kingdom) and then wrapped with a sterile bandage. At the end of the surgical treatment, the rats received an intramuscular dose of antibiotics (gentamycin sulphate, Italfarmaco, Milan, Italy; and amoxicillin clavulanic acid, Sandoz, Varese, Italy) and a fentanyl patch for pain relief for 5 days. To minimize possible risks of rejection due to the use of different species material (bovine collagen, human PRP), the animals received cyclosporine A 0.5 mg/kg (Sandimunn, Sandoz) the day before and during 5 days after surgery.

### Cell isolation

Transgenic bone marrow GFP-labeled MSCs were isolated from male GFP transgenic Lewis rats (RRRC, Columbia, MO), expanded and characterized as described previously.<sup>17</sup> GFP-labeled MSCs were analyzed for green fluorescence intensity at different passages in culture as well as for the expression of particular cell surface molecules using flow cytometry procedures: CD45-CyChrome™, CD11b-FITC (in order to quantify hematopoietic-monocytic contamination), CD90-PE, CD73-PE, CD44-PE (BD Pharmingen, San Diego, CA).

### Matrices

Integra (INTEGRA Bilayer Matrix Wound Dressing; Integra Lifesciences Corp.) is a bilayer membrane system used as a dermal regeneration template for skin replacement. It consists of a dermal layer made up of a porous matrix of bovine tendon collagen (92%) and chondroitin-6-sulfate (8%) with a mean pore diameter ranging from 30 to 120  $\mu$ m and a global porosity of 98%. The epidermal substitute layer is made up of synthetic polysiloxane polymer. In some experiments, Integra was adsorbed with PRP to obtain a recently patented bioengineered scaffold, Ematrix, 3 hours before experiments. Ematrix, is a patent belonging to AOUC Careggi Hospital (FI2008A000070), invented by C. Mirabella. PRP was obtained by plateletpheresis from the whole blood of adult healthy volunteers after receiving an informed consent and centrifuged at 2,012 g for 10 minutes; the platelets were next leucodepleted, irradiated, and counted automatically using a hematology analyzer. PRP was activated with a solution of thrombin and calcium chloride (1 : 10) and then dropped on the dermal layer of Integra matrix stirred and left until gel formation; the final platelet concentration within the matrix was of  $1.2 \times 10^6/\mu$ L of PRP.<sup>30</sup>

### Cell seeding

Rat GFP-labeled MSCs were grown in Dulbecco's modified Eagle medium (DMEM) supplemented with 20% fetal bovine serum, 2-mM L-glutamine, 100 U/mL penicillin/streptomycin

(Sigma, Milan, Italy) at 37 °C in a humidified atmosphere of 5% CO<sub>2</sub>. Subconfluent cells were washed with PBS twice, detached with trypsin/EDTA, counted, and expanded in plastic adherence before being used for the experiments on Integra and Ematrix. In order to obtain a homogeneous population avoiding hematopoietic contamination, cells at passage P4-P5 were used for all of the experiments. Rat GFP-labeled MSCs ( $1 \times 10^6$  cells) were dropped on the dermal layers of scaffolds 24 hours before the surgical treatment. Unseeded matrices (Integra and Ematrix) were used as control matrices.

### Morphological analysis

Wound punch biopsies (2 × 4 mm) were obtained from the anesthetized rats after 7, 14, and 28 days from wounding. Bioptic fragments were taken after removing the polysiloxane layer and allowing a 2-mm border of implanted scaffold to be left around the edge of the wound. The specimens were, then, fixed in 10% buffered formalin, dehydrated in alcohol, cleared in xylene, and embedded in paraffin. Sections 8 μm thick were stained with hematoxylin and eosin and observed under a light microscope. Parallel samples were fixed in 4% paraformaldehyde in PBS overnight, then transferred to PBS containing 30% sucrose and finally frozen at -80 °C. Cryostat sections, 10 μm thick, were permeabilized with cold acetone for 10 minutes, blocked with a solution containing 0.5% bovine serum albumin (Sigma) and 0.2% gelatin in PBS for 30 minutes, and then incubated at 4 °C overnight with the following antibodies: mouse monoclonal anti-GFP rhodamine (1 : 200; Santa Cruz Biotechnology, Heidelberg, Germany), mouse monoclonal anti-pan-cytokeratin (1.50; Leica Biosystems, Milan, Italy), rabbit polyclonal anti-Ki67 (1 : 100; Abcam, Cambridge, UK), mouse monoclonal anti-CD31 (1 : 50; Dako, Milan, Italy), rabbit polyclonal anti-MMP2 (1 : 200; Abcam), and rabbit polyclonal anti-matrix metalloproteinase 9 (MMP9; 1 : 100; Abcam). The immunoreactions were revealed by incubation with specific anti-mouse Alexa Fluor 488-conjugated IgG, anti-rabbit Alexa Fluor 488-conjugated IgG, or anti-rabbit Alexa Fluor 568-conjugated IgG (1 : 200; Molecular Probes Inc., Eugene, OR) for 1 hour at RT. In some experiments, counterstaining was performed with Syto16 (1 : 1,000; Molecular Probes Inc.) to reveal nuclei. After washing in PBS, the sections were mounted with an antifade mounting medium (Biomedica Gel mount, Electron Microscopy Sciences, Foster City, CA). A negative control was performed by replacing the primary antibody with nonimmune mouse serum. Sections were examined with a Leica TCS SP5 confocal laser scanning microscope (Leica Microsystems, Mannheim, Germany) equipped with a HeNe/Argon laser source for fluorescence measurements. Fluorescence was collected using a Leica PlanApo X63 oil-immersion objective. Optical sections (1,024 × 1,024 pixels; Leica Microsystems) at intervals of 0.8 μm were obtained and superimposed to create a single composite image.

When needed, a single optical fluorescent section and DIC images were merged to better define the localization of immunofluorescent signals. The mean number of MSCs was counted in 10 optical field (35,000 μm<sup>2</sup>) per section (three per group) from biopsies of animals treated with MSC-seeded Integra and Ematrix.

Quantification of pan-cytokeratin and Ki67<sup>+</sup> cells, CD31<sup>+</sup> blood vessels, and densitometric analysis of the intensity of MMP2 and MMP9 fluorescent signal was performed on digi-

tized images using ImageJ software (<http://imagej.nih.gov/ij/>) in 20 regions of interest of 100 μm<sup>2</sup> for each confocal stack (at least 10). The number of CD31-positive microvessels in the dermal layer was also quantified in 10 optical field (13,000 μm<sup>2</sup>) per section (three per group) from biopsies of each group of animals.

The evaluation of tissue fibrosis was carried out on cryostat sections (10 μm thick) fixed in paraformaldehyde vapors and stained with Van Gieson method for collagen.<sup>31</sup> The subepidermal collagen deposition was calculated as percentage of area covered by collagen out of the total subepidermal area. The mean epithelial thickness as well as the number of hair follicles was evaluated in 10 optical field (2.16 mm<sup>2</sup>) per section (three per group) from biopsies of each group of animals.

### Clinical evaluation

All the animals were monitored daily for weight and matrix conditions to exclude possible infection or loss of matrix.

### Statistical analysis

Each experiment was performed in triplicate, and the data obtained were reported as mean ± SEM; statistical significance was determined by Student's *t* test or one-way ANOVA and Newman-Keuls multiple comparison test (if more than two groups were compared). A *p* value < 0.05 was considered as significant. Calculations were performed using GraphPad Prism software (GraphPad, San Diego, CA).

## RESULTS

Clinical examination revealed that the full-thickness wounds treated with MSC-seeded Integra and Ematrix showed accelerated healing as compared with the untreated, Integra and Ematrix-treated groups. In particular, in the animals treated with the MSC-seeded matrices, the wounds appeared completely reepithelialized and showed an evident return of hair follicles (see Figure 1C). Confocal microscopic evaluation showed that both the unseeded and MSC-seeded scaffolds (Integra and Ematrix) were fully integrated into the host skin since the early times (7–14 days) postwounding, as judged by their complete colonization by rat tissues (Figure 2). Giant histiocytes (foreign body reaction) were sometimes observed within the pores of the seeded matrices at both 7 and 14 days postwounding (data not shown).

To determine the persistence of MSCs within the pores of the engrafted matrices, we analyzed wounds for MSC content using GFP as a cell marker. It was found that the amount of GFP<sup>+</sup> cells within the Ematrix was significantly higher as compared with that of Integra (Figure 2), consistent with our previous observations that Ematrix provides a better microenvironment to suit the need and influence MSC functions.<sup>30</sup> In both the experimental conditions, the cells were found intermingled with the surrounding host cells (Figure 2).

We also showed that wounds in the animals treated with MSC-seeded Integra and Ematrix matured faster than wounds in untreated or Integra and Ematrix-treated animals. In particular, the healing process was characterized by an initial inflammatory phase (soon after injury), followed by



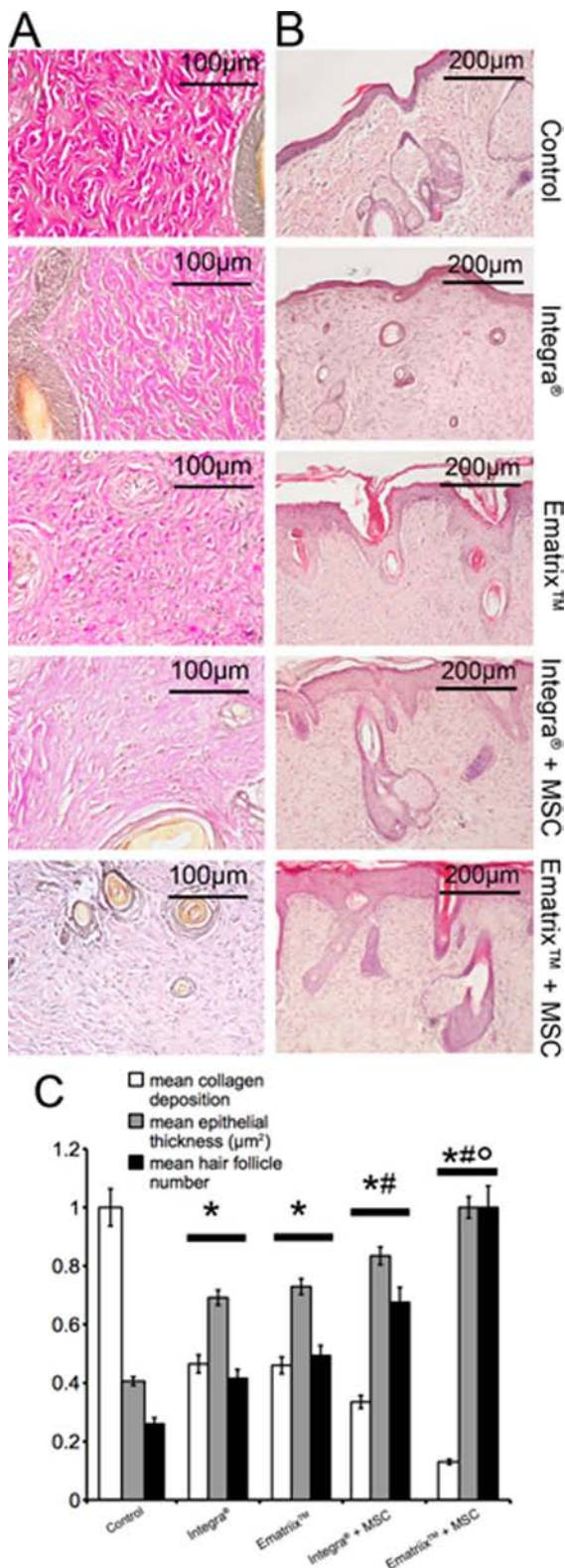


**Figure 1.** MSC-seeded matrices improve the quality of regenerated skin in rats. Representative light microscopy images of regenerated skin from each group of animals taken at day 28 postinjury (A,B). Tissues were excised from the wounded area, fixed in paraformaldehyde or formalin, and stained with Van Gieson method for collagen (A) or hematoxylin and eosin (H&E) (B). In the histogram C, the mean collagen content, epidermal thickness, and hair follicle number in untreated and treated wounds are reported. Significance of differences among untreated and treated groups was evaluated by one-way ANOVA. Values are reported as mean ± SEM. \**p* < 0.05 vs. control, #*p* < 0.05 vs. Integra, °*p* < 0.05 vs. Integra + MSC.

formation and maturation of a granulation tissue, extracellular matrix remodeling, and new tissue formation (epidermal and skin appendage regeneration at the end of the observation period, at day 28, see Figure 1C). In the animals treated with the cell bioengineered scaffolds, the wound underwent a faster maturation/remodeling phase, characterized by vascular progression and increased expression of MMP9 (Figure 3) in the wound bed 14 days after surgery. Instead, MMP2 expression did not vary in the extracellular matrix of the animals treated with Integra or Ematrix-MSCs (data not shown). Of interest, the presence of MSC within the matrices also greatly ameliorated the quality of the regenerated skin at day 28 postwounding; indeed, the treatment with MSC-Integra and in particular with MSC-Ematrix led to a significant collagen remodeling, decreased collagen deposition by Van Gieson staining within the neo-formed tissue (Figure 1A,C) as compared with the untreated wounds and those treated with the unseeded matrices, including Ematrix. Moreover, MSC-seeded matrices induced enhanced reepithelialization, characterized by a thicker multilayered epidermis, a greater return of hair follicles and sebaceous glands (Figure 1B), and enhanced blood vessel formation, as detected by immunofluorescent staining of CD31, an established marker for endothelial cells (Figure 4). By 28 days, Integra and Ematrix became more difficult to visualize, being apparently incorporated into the newly formed skin tissues. Moreover, the transplanted cells were still visible inside the scaffolds, although in reduced number; these cells were mainly located within the dermis with some of them migrating into the epidermal structures, such as the repaired epithelium and sebaceous glands (Figure 5A,B).

To test whether the engrafted MSCs, beside contributing to the recreation of a suitable microenvironment for wound repair through paracrine signaling, were able to trans-differentiate into the skin cell types, the cells were double immunostained for the expression of GFP and pan-cytokeratin, a marker of epithelial cell differentiation. The results showed that none of the engrafted MSCs expressed pan-cytokeratin 28 days postinjury, suggesting that the transplanted cells were unable to differentiate within the cutaneous wounds, in our experimental conditions (Figure 6A–E). Consistent with this, the engrafted cells displayed a quite immature phenotype, showing a round-shaped morphology. Moreover, most of these cells resulted negative for Ki67 a cell cycle marker, indicating that the wound environment was not suitable for promoting cell proliferation in the exogenously delivered MSCs (Figure 6F). Interestingly, GFP<sup>+</sup>/pan-cytokeratin<sup>+</sup> cells were observed inside the pores of the matrices in the proximity of GFP<sup>+</sup>-MSCs in the earlier phase of

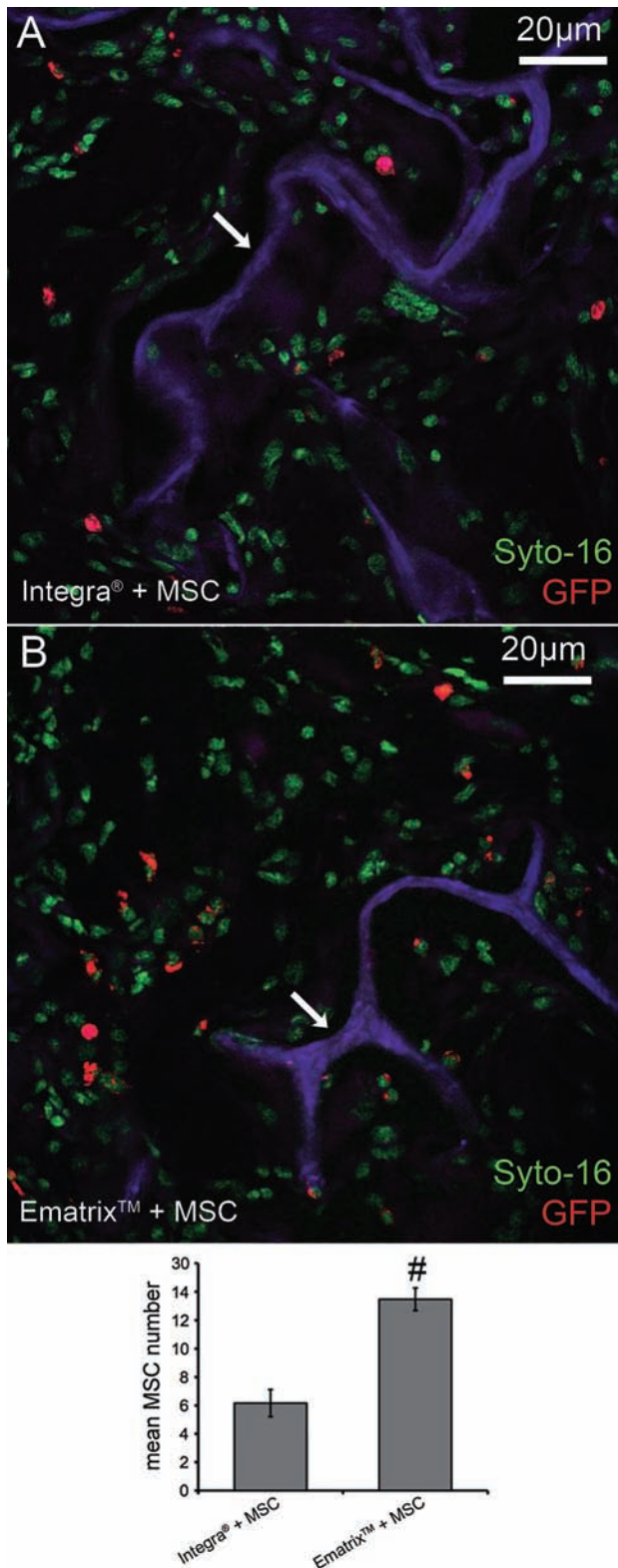


**Figure 2.** MSC-seeded matrices are incorporated into the cutaneous wounds in rats. Representative confocal images of wounds after 14 days from the application of the bioengineered matrices (A,B). Tissues were excised from the wounded area, fixed in paraformaldehyde, and stained with antibodies against green fluorescent protein (GFP) recognizing GFP-MSCs (red) and Syto16 to reveal nuclei (green). The dermal matrices offer high autofluorescence (arrows). In the histogram, the mean number of MSCs inside the pores of the matrices is reported. Significance of differences among treated groups was evaluated by *t* test. Values are reported as mean  $\pm$  SEM. <sup>#</sup>*p* < 0.05.

wound healing (day 14 after transplantation; Figure 6B–E,G). These cells were also observed within the transplanted unseeded matrices but were present in higher amount within the bioengineered matrices (MSC-Integra and MSC-Ematrix), providing evidence for a role of MSCs in the recruitment of epithelial cells at the sites of skin regeneration. To further clarify the nature of these cells, they were immunostained to detect the cell cycle-associated antigen Ki67. The findings shown in Figure 6F–H showed that about 40% of the cells positive for cytokeratin expressed Ki67 within their nuclei, suggesting that the cells migrating into the matrix pores represented endogenous epithelial precursors in different stages of differentiation, likely recruited by MSCs at these sites to participate in tissue regeneration.

## DISCUSSION

In the present study, we have demonstrated that the use of bioengineered scaffolds containing MSCs in combination or not with a mixture of growth factors (MSCs-Integra and MSCs-Ematrix) greatly ameliorates the quality of cutaneous repair.

Indeed, the animals receiving MSC-seeded Integra scaffold showed increased reepithelization and angiogenesis, reduced dermal collagen content, and a greater return of skin appendages, as compared with those treated with the unseeded matrices, including Ematrix. The therapeutic benefits were particularly evident when the wounds were treated with MSCs seeded on PRP-enriched scaffold, Ematrix, indicating that the incorporation of growth factors within the pores of the bioengineered scaffolds offered additional therapeutic advantages over the presence of MSCs, including the augmentation of MSC survival and stemness, as also previously demonstrated.<sup>30</sup> One of the possible mechanisms involved can reside in the presence of a fibrin network, deriving from platelet activation, that can act as a scaffold to sequentially deliver different growth factors important in the process of wound healing.<sup>32</sup> We have previously shown<sup>18</sup> that the contribution of MSCs to skin repair/regeneration was due to their capacity to secrete paracrine signals, such as growth factors and cytokines, which are relevant for tissue repair/regeneration.<sup>12,13,16,18,30,33</sup> Indeed, we found that the expression of MMP9, a major factor released by MSCs,<sup>31–34</sup> was significantly increased in the wound bed of the animals treated with MSC-seeded matrices. This is an important finding as MMPs are key regulatory molecules in the remodeling and degradation of extracellular matrix component. Their up-regulated expression/activity represents an important event during



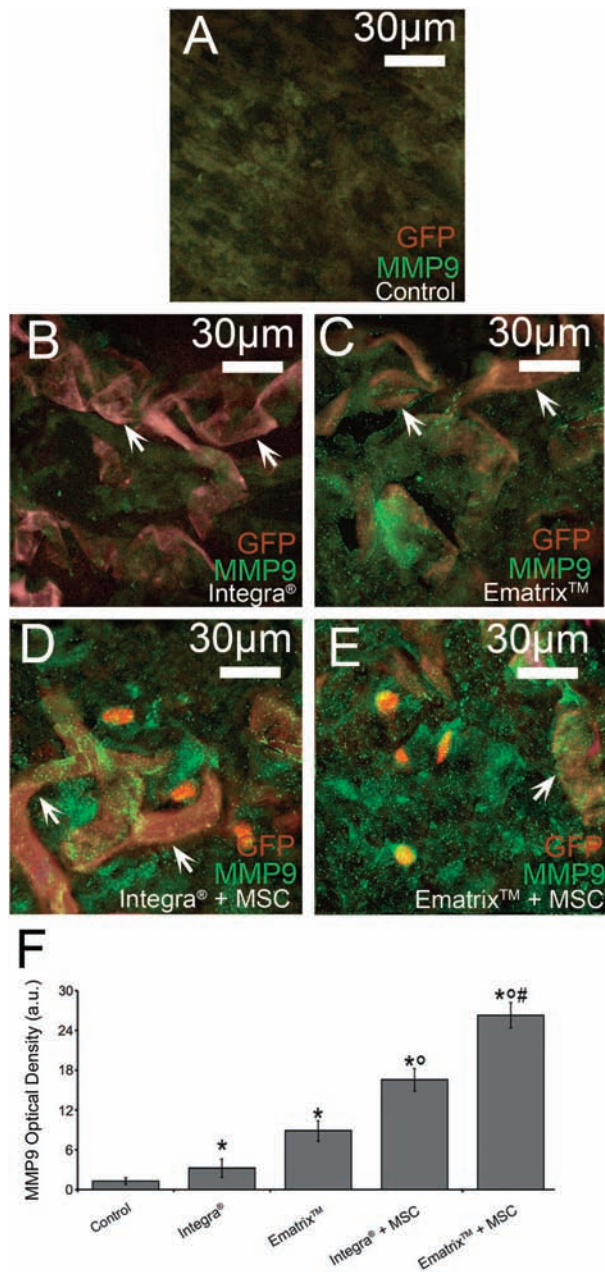


**Figure 3.** MSC-seeded matrices increase MMPs expression. Representative confocal images of wound healing from each group of the treated animals taken at day 14 postinjury (A–E). Tissues were excised from the wounded area, fixed in paraformaldehyde, and stained with antibodies against MMP9 (green) and GFP to reveal GFP-MSCs (red). Note that MMP9 is expressed in the ECM, inside the engrafted MSCs and in the close proximity of the meshes. The dermal matrices are indicated with arrows. The quantitative analysis of MMP9 expression is reported in the histogram (F). Significance of differences among untreated and treated groups were evaluated by *t* test. Values are reported as mean ± SEM. \**p* < 0.05 vs. control, °*p* < 0.05 vs. Integra, #*p* < 0.01 vs. Integra + MSC.

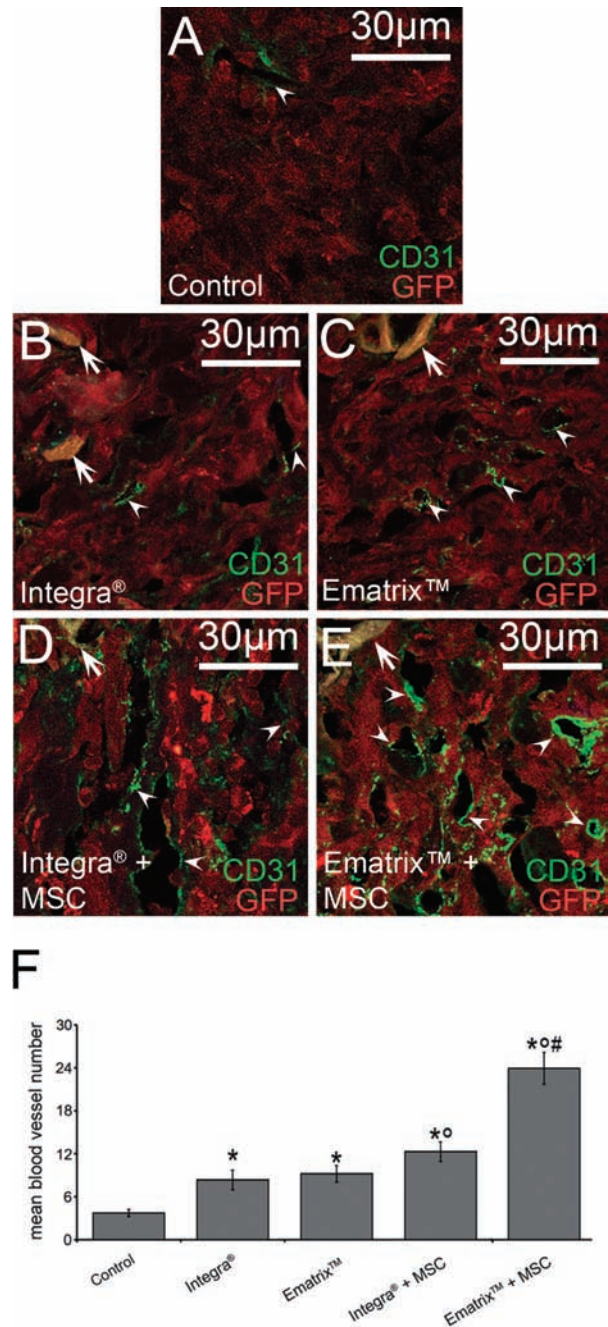


**Figure 4.** MSC-seeded matrices increase neo-vascularization of regenerated skin in rats. Representative confocal images of wounds at day 28 postinjury (A–E). Tissues were excised from the wounded area, fixed in paraformaldehyde, and stained with antibodies against CD31, recognizing endothelial cells (green) and antibodies against GFP, to reveal GFP-MSCs. The dermal matrices are indicated with arrows. The quantitative analysis of CD31 positive microvessels (arrowheads) is reported in the histograms (F). Significance of differences among untreated and treated groups was evaluated by *t* test. Values are reported as mean ± SEM. \**p* < 0.05 vs. control, °*p* < 0.05 vs. Integra, #*p* < 0.01 vs. Integra + MSC.

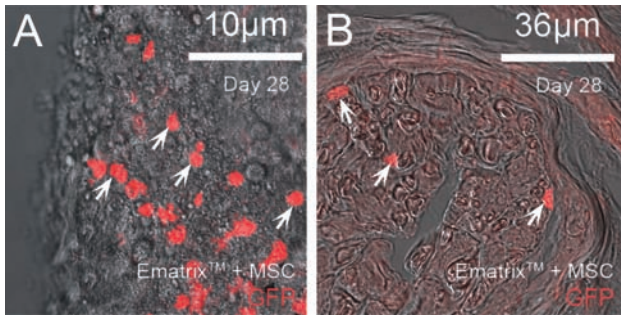
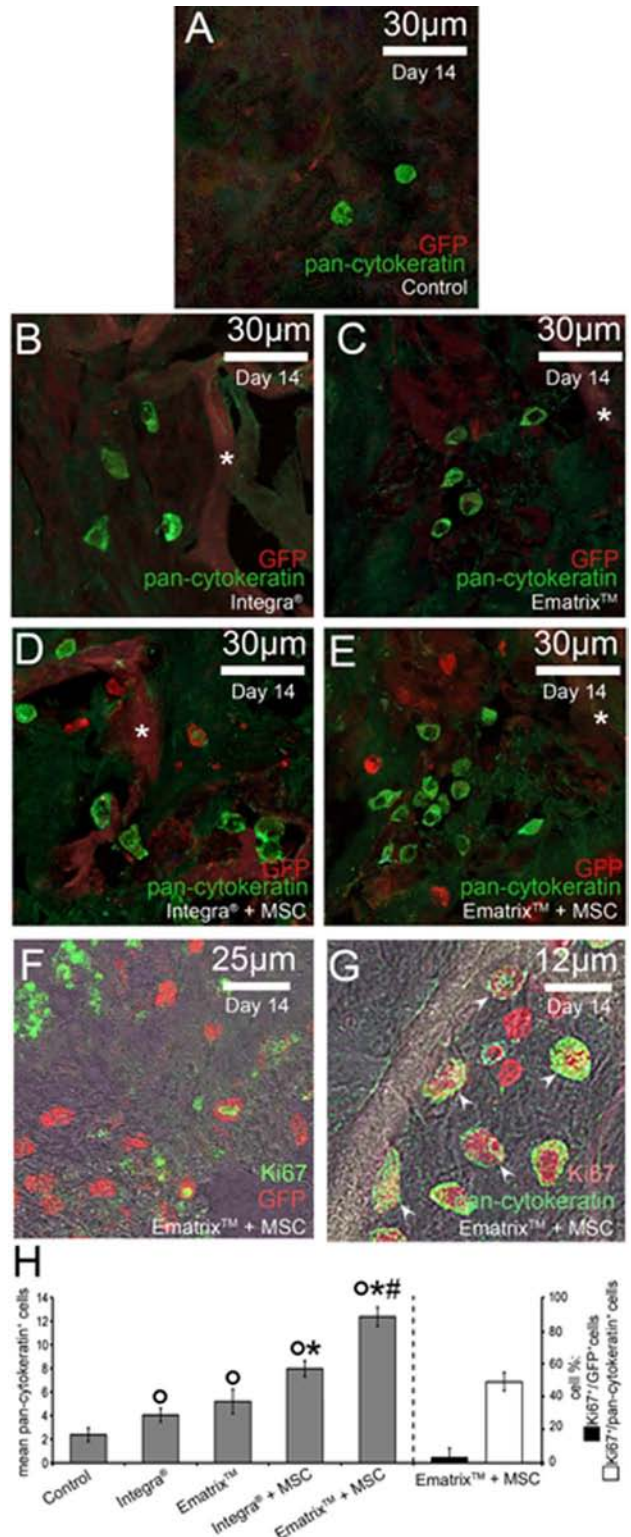


**Figure 5.** MSCs migration in wounds. Representative confocal images of wound healing from MSCs-Ematrix-treated rats superimposed on DIC images. Tissues were excised from the wounded area, fixed in paraformaldehyde, and stained with antibodies against GFP (A,B) to detect engrafted MSCs at day 28 postinjury. The presence of MSCs within the epidermal layer and sebaceous glands is indicated with arrows.

**Figure 6.** MSCs differentiation in wounds. Representative confocal images of wound healing from each group of the treated animals. Tissue was excised from wounded area 14 days postinjury and double stained with anti-GFP (red) and pan-cytokeratin antibodies (green, A–E) to assess epithelial differentiation. Note that no double-positive cells are identified to denote cell differentiation by MSCs. The dermal matrices are indicated with asterisks. Sections were also stained for GFP (red) and Ki67 (green) (F) and pan-cytokeratin (green) and Ki67 (red), to detect cell proliferation by the endogenous precursors (G). Double staining for pan-cytokeratin and Ki67 (arrowheads) in treated animals with MSC-seeded matrix shows the presence of replicating epithelial precursors inside the meshes. In F and G, the confocal images were superimposed to DIC images. In the histogram (H), the mean number of recruited pan-cytokeratin<sup>+</sup> cells as well as the percentage of Ki67 expressing cells on the total number of GFP<sup>+</sup> cells and the percentage of Ki67<sup>+</sup> on the total number of pan-cytokeratin<sup>+</sup> cells in the treated wounds are reported. Significance of differences among treated groups was evaluated by *t* test and one-way ANOVA. Values are reported as mean ± SEM. °*p* < 0.01 vs. control, \**p* < 0.05 vs. Integra, #*p* < 0.05 vs. Integra + MSC.



tissue regeneration and skin wound healing,<sup>35,36</sup> limiting the progression of pathological fibrosis and the loss of skin function.<sup>25,26</sup> Moreover, the animals receiving the cell bioengineered matrices showed increased vascularization of the wound bed, likely due to the release of VEGF and FGF by the transplanted MSCs. Finally, the paracrine action of MSCs on wound healing was also supported by data showing that MSCs, although perfectly integrated with the other connective tissue cells, retained an undifferentiated morphology and did not express pan-cytokeratin, an epithelial cell marker, suggesting to be unable to transdifferentiate into the wound tissue in our experimental conditions. This result is in contrast with other reports in the literature showing epidermal differentiation by MSCs. However, most of these studies came from *in vitro* experiments, where cells were forced to differentiate in optimized induction media,<sup>11,37</sup> which are of unclear



relevance to the actual differentiation potential in vivo. Moreover, the fact that epithelial transdifferentiation in MSCs is a limited and rare event in vivo,<sup>9,10</sup> given also the small amount of cells retained soon after the inoculation, questions the real contribution of this process to the therapeutic benefits observed following MSC transplantation.

Another important observation of this study was that MSCs, therapeutically applied to wound, enhanced the recruitment of the endogenous epithelial precursors to the sites of injury; GFP/pan-cytokeratin<sup>+</sup> cells were, in fact, found within the pores of the scaffolds in the close proximity of GFP<sup>+</sup>-MSCs, particularly in the animals treated with MSC-Ematrix, suggesting the possibility of a crosstalk between resident epithelial precursors and the transplanted MSCs in the injured tissue. Some of the GFP/pan-cytokeratin<sup>+</sup> cells coexpressed Ki67, a marker of cell cycle, indicating epithelial proliferation. Taking into consideration our previous in vitro observations showing that MSCs stimulate proliferation of stem/precursor cells by paracrine and direct cell contact-mediated interaction,<sup>18,30</sup> the present data expand their biological effects on stem cell function, suggesting a role for these cells in stimulating migration of endogenous epidermal precursors at the sites of tissue repair/regeneration. Indeed, lineage tracing experiments and functional skin reconstitution studies in mice have unambiguously showed that the interfollicular epidermis<sup>38</sup> and the upper constant region of hair follicles<sup>39</sup> contain cells with stem cell properties. It is, therefore, tempting to speculate that transplanted MSCs may favorably imprint the local microenvironment to support the endogenous mechanisms of cutaneous repair/regeneration. On the other hand, we have also shown, in the present study, that engrafted MSCs did not proliferate and their number decreased gradually during the healing progression, in agreement with previous reports.<sup>40</sup> This phenomenon represents a critical challenge encountered in stem cell therapy, which may greatly limit their therapeutic efficacy. It is generally assumed that the loss of engrafted cells is due to the hostile microenvironment of the cutaneous wound, making it difficult for the exogenously delivered stem cells to engraft and survive. Hence, a major focus in this field is to better understand how stem cells respond to the host environment and to identify strategies to enhance MSCs survival and maintain their beneficial effects on cutaneous wound repair/regeneration.

In conclusion, the results of this study provide strong evidence that transplantation with MSCs seeded on suitable biological scaffolds may constitute a promising therapeutic strategy for the treatment of skin injury. We propose that MSCs exert a trophic effect on skin wound healing, which assist and control the host repair/regenerative mechanisms. A better understanding of the mechanisms mediating the crosstalk between the injected cells and resident cells may be relevant for designing therapeutic protocols for skin regeneration after injury and disease and bridge the gap between preclinical and clinical findings.

## ACKNOWLEDGMENTS

**Source of Funding:** This work was partially supported by grants of MIUR (ex 60%) to SZ-O and LF, and Ente Cassa di Risparmio Firenze to LF.

**Conflicts of Interest:** The authors certify that there is no conflict of interest with any financial organization regarding the material discussed in the manuscript.

## REFERENCES

- Zhang H, Song P, Tang Y, Zhang XL, Zhao SH, Wei YJ, et al. Injection of bone marrow mesenchymal stem cells in the borderline area of infarcted myocardium: heart status and cell distribution. *J Thorac Cardiovasc Surg* 2007; 134: 1234–40.
- Baiguera S, Jungebluth P, Mazzanti B, Macchiarini P. Mesenchymal stromal cells for tissue-engineered tissue and organ replacements. *Transpl Int* 2012; 25: 369–82.
- Yi T, Song SU. Immunomodulatory properties of mesenchymal stem cells and their therapeutic applications. *Arch Pharm Res* 2012; 35: 213–21.
- Jeon YK, Jang YH, Yoo DR, Kim SN, Lee SK, Nam MJ. Mesenchymal stem cells interaction with skin wound-healing effect on fibroblast cells and skin tissue. *Wound Repair Regen* 2010; 18: 655–61.
- Wu Y, Huang S, Enhe J, Fu X. Insights into bone marrow-derived mesenchymal stem cells safety for cutaneous repair and regeneration. *Int Wound J* 2012; 9: 586–94.
- McFarlin K, Gao X, Liu YB, Dulchavsky DS, Kwon D, Arbab AS, et al. Bone marrow-derived mesenchymal stromal cells accelerate wound healing in the rat. *Wound Repair Regen* 2006; 14: 471–8.
- Wu Y, Zhao RC, Tredget EE. Concise review: bone marrow-derived stem/progenitor cells in cutaneous repair and regeneration. *Stem Cells* 2010; 28: 905–15.
- Zou Z, Zhang Y, Hao L, Wang F, Liu D, Su Y, et al. More insight into mesenchymal stem cells and their effects inside the body. *Expert Opin Biol Ther* 2010; 10: 215–30.
- Li H, Fu X, Ouyang Y, Cai C, Wang J, Sun T. Adult bone-marrow-derived mesenchymal stem cells contribute to wound healing of skin appendages. *Cell Tissue Res* 2006; 326: 725–36.
- Sasaki M, Abe R, Fujita Y, Ando S, Inokuma D, Shimizu H. Mesenchymal stem cells are recruited into wounded skin and contribute to wound repair by transdifferentiation into multiple skin cell type. *J Immunol* 2008; 180: 2581–7.
- Ma K, Laco F, Ramakrishna S, Liao S, Chan CK. Differentiation of bone marrow-derived mesenchymal stem cells into multi-layered epidermis-like cells in 3D organotypic coculture. *Biomaterials* 2009; 30: 3251–8.
- Chen L, Tredget EE, Wu PY, Wu Y. Paracrine factors of mesenchymal stem cells recruit macrophages and endothelial lineage cells and enhance wound healing. *PLoS ONE* 2008; 3: e1886. doi: 10.1371/journal.pone.0001886.
- Hocking AM, Gibran NS. Mesenchymal stem cells: paracrine signaling and differentiation during cutaneous wound repair. *Exp Cell Res* 2010; 316: 2213–19.
- Li H, Fu X. Mechanisms of action of mesenchymal stem cells in cutaneous wound repair and regeneration. *Cell Tissue Res* 2012; 348: 371–7.
- Lee SH, Jin SY, Song JS, Seo KK, Cho KH. Paracrine effects of adipose-derived stem cells on keratinocytes and dermal fibroblasts. *Ann Dermatol* 2012; 24: 136–43.
- Jiang D, Jiang D, Qi Y, Walker NG, Sindrilaru A, Hainzl A, et al. The effect of adipose tissue derived MSCs delivered by a chemically defined carrier on full-thickness cutaneous wound healing. *Biomaterials* 2013; 34: 2501–15.
- Sassoli C, Pini A, Mazzanti B, Quercioli F, Nistri S, Saccardi R, et al. Mesenchymal stromal cells affect cardiomyocyte growth through juxtacrine Notch-1/Jagged-1 signaling and paracrine mechanisms: clues for cardiac regeneration. *J Mol Cell Cardiol* 2011; 51: 399–408.



18. Sassoli C, Pini A, Chellini F, Mazzanti B, Nistri S, Nosi D, et al. Bone marrow mesenchymal stromal cells stimulate skeletal myoblast proliferation through the paracrine release of VEGF. *PLoS ONE* 2012; 7: e37512. doi: 10.1371/journal.pone.0037512.
19. Yoon BS, Moon JH, Jun EK, Kim J, Maeng I, Kim JS, et al. Secretory profiles and wound healing effects of human amniotic fluid-derived mesenchymal stem cells. *Stem Cells Dev* 2010; 19: 887–902.
20. Caplan AI, Dennis JE. Mesenchymal stem cells as trophic mediators. *J Cell Biochem* 2006; 98: 1076–84.
21. Seifert AW, Monaghan JR, Voss SR, Maden M. Skin regeneration in adult axolotls: a blueprint for scar-free healing in vertebrates. *PLoS ONE* 2012; 7: e32875. doi: 10.1371/journal.pone.0032875.
22. Tammela T, Enholm B, Alitalo K, Paavonen K. The biology of vascular endothelial growth factors. *Cardiovasc Res* 2005; 65: 550–63.
23. Stevens LJ, Page-McCaw A. A secreted MMP is required for re-epithelialization during wound healing. *Mol Biol Cell* 2012; 23: 1068–79.
24. Kahari VM, Saarialho-Kere U. Matrix metalloproteinases in skin. *Exp Dermatol* 1997; 6: 199–213.
25. Zhang ZF, Zhang YG, Hu DH, Shi JH, Liu JQ, Zhao ZT, et al. Smad interacting protein 1 as regulator of skin fibrosis in pathological scars. *Burns* 2011; 37: 665–72.
26. Sidgwick GP, Bayat A. Extracellular matrix molecules implicated in hypertrophic and keloid scarring. *J Eur Acad Dermatol Venereol* 2012; 26: 141–52.
27. Kramann R, DiRocco DP, Humphreys BD. Understanding the origin, activation and regulation of matrix-producing myofibroblasts for treatment of fibrotic disease. *J Pathol* 2013; 231: 273–89.
28. Rustad KC, Wong VW, Sorkin M, Glotzbach JP, Major MR, Rajadas J, et al. Enhancement of mesenchymal stem cell angiogenic capacity and stemness by a biomimetic hydrogel scaffold. *Biomaterials* 2012; 33: 80–90.
29. Prestwich GD, Erickson IE, Zarembinski TI, West M, Tew WP. The translational imperative: making cell therapy simple and effective. *Acta Biomater* 2012; 8: 4200–7.
30. Formigli L, Benvenuti S, Mercatelli R, Quercioli F, Tani A, Mirabella C, et al. Dermal matrix scaffold engineered with adult mesenchymal stem cells and platelet-rich plasma as a potential tool for tissue repair and regeneration. *J Tissue Eng Regen Med* 2012; 6: 125–34.
31. Formigli L, Perna AM, Meacci E, Cinci L, Margheri M, Nistri S, et al. Paracrine effects of transplanted myoblasts and relaxin on post-infarction heart remodeling. *J Cell Mol Med* 2007; 11: 1087–100.
32. Wilcke I, Lohmeyer JA, Liu S, Condurache A, Krüger S, Mailänder P, et al. VEGF(165) and bFGF protein-based therapy in a slow release system to improve angiogenesis in a bioartificial dermal substitute in vitro and in vivo. *Langenbecks Arch Surg* 2007; 392: 305–14.
33. Gneccchi M, Zhang Z, Ni A, Dzau VJ. Paracrine mechanisms in adult stem cell signaling and therapy. *Circ Res* 2008; 103: 1204–19.
34. Lee T. Host tissue response in stem cell therapy. *World J Stem Cells* 2010; 2: 61–6.
35. Alameddine HS. Matrix metalloproteinases in skeletal muscles: friends or foes? *Neurobiol Dis* 2012; 48: 508–18.
36. Bhattacharyya S, Fang F, Tourtellotte W, Varga J. Egr-1: new conductor for the tissue repair orchestra directs harmony (regeneration) or cacophony (fibrosis). *J Pathol* 2013; 229: 286–97.
37. Păunescu V, Deak E, Herman D, Siska IR, Tănăsie G, Bunu C, et al. In vitro differentiation of human mesenchymal stem cells to epithelial lineage. *J Cell Mol Med* 2007; 11: 502–8.
38. Doupe DP, Klein AM, Simons BD, Jones PH. The ordered architecture of murine ear epidermis is maintained by progenitor cells with random fate. *Dev Cell* 2010; 18: 317–23.
39. Blanpain C, Lowry WE, Geoghegan A, Polak L, Fuchs E. Self-renewal, multipotency, and the existence of two cell populations within an epithelial stem cell niche. *Cell* 2004; 118: 635–48.
40. Saraswati S, Deskins DL, Holt GE, Young PP. Pyrvinium, a potent small molecule Wnt inhibitor, increases engraftment and inhibits lineage commitment of mesenchymal stem cells (MSCs). *Wound Repair Regen* 2012; 20: 185–93.